Progress In Electromagnetics Research C, Vol. 36, 69–79, 2013

UNIQUE-PLANAR VIALESS MARCHAND BALUN WITH NOVEL METHOD OF MEASUREMENT

Yu Ye[1, 2, *], Lingyun Li[1], Hao Sun[1], and Xiaowei Sun[1]

[1]Key Laboratory of Terahertz Solid-State Technology, Shanghai Institute of Microsystem and Information Technology, Shanghai 200050, China

[2]Graduate University of Chinese Academy of Sciences, Beijing 100049, China

Abstract—A unique-planar vialess Marchand balun for V-band application is presented. The balun can achieve less than 2° phase imbalance and 0.3 dB amplitude imbalance from 54 GHz to 66 GHz, with the insertion losses of −3.6 dB and −3.9 dB for the two balanced ports and the return loss of less than −15 dB in the unbalanced port. The novel back-to-back measured method has been proposed and analyzed, the amplitude and phase imbalances can be derived from the measured back-to-back two-port scattering results. The extracted results achieve good agreement with the single balun simulation, with no more than 0.15 dB and 1° amplitude and phase differences. This balun configuration and the measurement method can simplify the fabrication, achieve good yield, ease the assembling and decrease the cost.

1. INTRODUCTION

Recently, millimeter-wave wireless systems have draw great demands on balanced circuits, such as push-pull amplifiers, balanced mixers and balanced multipliers [1–4]. In such balanced circuits, the Marchand baluns have been widely used in single and differential signal transition for their ease of implementation and steady performance [5–7]. However, most of these Marchand baluns require via-holes at the isolation ports, which result in some issues, such as complexity in fabrication, bad yielding as well as parasitic effects of via-holes to the balun electrical performance, and also the cost [8–10]. Especially in

Received 25 November 2012, Accepted 28 December 2012, Scheduled 9 January 2013
* Corresponding author: Yu Ye (yye@mail.sim.ac.cn).

millimeter-wave frequencies such as V-band and W-band applications, the parasitic effects of via-holes are key issues for Marchand balun performance consideration, such as amplitude and phase balances.

The conventional Marchand balun measurements are commonly implemented by three-port or four-port scattering testing equipments. In three-port measurement, one of the three ports connects to a $50\,\Omega$ calibration device, which will result uncertain impedance deviations in this port terminal for this port could not be exactly calibrated, which is more crucial in higher millimeter-wave frequencies. Although four-port testing method can solve this problem, these testing equipments are much more expensive than two-port equipments, which increases the testing cost of millimeter-wave devices. Cost is a hurdle for devices in commercial application.

Over the past years, several vialess baluns have been reported, such as multi-section vialess baluns and CPW baluns [11–13]. Most of them have the backside ground apertures, which result difficulties in assembling and increase the fabrication complexity and cost. Moreover, the CPW baluns have the surface ground connection problems, which are serious in higher millimeter-wave frequencies. In some other planar baluns, such as [14, 15], although the designs avoid those issues mentioned above, the need of wire-bonding or the bulky size make them unattractive in millimeter-wave applications.

In this paper, a planar vialess Marchand balun facilitating the fabrication and assembling has been presented and a novel back-to-back measured method has been proposed for saving the cost of balun testing, in which expensive four-port equipment can be substituted by two-port equipment. Two microwave radial stubs have been employed to realize vialess configuration. In addition, it can provide DC isolation in all three ports, which the Marchand balun with via-holes could not serve. The paper is organized as follow. A novel back-to-back measured method has been proposed and analyzed in Section 2. Section 3 describes the vialess balun configuration and the experimental results. Conclusions are drawn in Section 4.

2. PROPOSED BACK-TO-BACK MEASUREMENT METHOD

As shown in Figure 1, "1" represents the unbalanced port of the Marchand balun, where "2" and "3" are the two balanced port. The Marchand core consists of two coupled sections, each of which is one quarter-wavelength long at the center frequency of operation. The coupling factor of couplers is C and the three ports are all terminated with the same impedance. As in [16, 17], the theoretical scattering

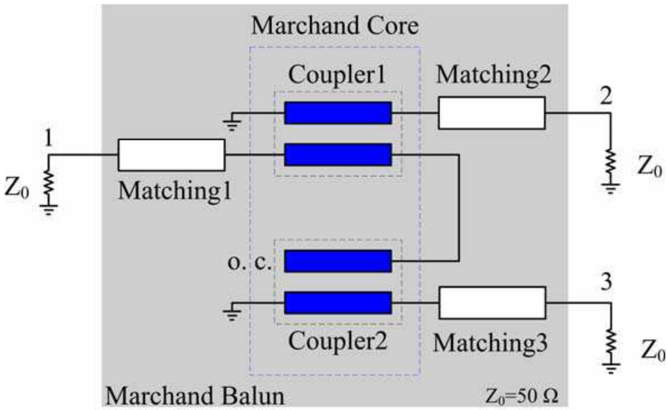

Figure 1. Block diagram of a Marchand balun as two identical couplers with port impedance matching.

matrix, $[S]_{core}$, can be given by,

$$[S]_{core} = \begin{bmatrix} \frac{1-3C^2}{1+C^2} & j\frac{2C\sqrt{1-C^2}}{1+C^2} & -j\frac{2C\sqrt{1-C^2}}{1+C^2} \\ j\frac{2C\sqrt{1-C^2}}{1+C^2} & \frac{1-C^2}{1+C^2} & \frac{2C^2}{1+C^2} \\ -j\frac{2C\sqrt{1-C^2}}{1+C^2} & \frac{2C^2}{1+C^2} & \frac{1-C^2}{1+C^2} \end{bmatrix}. \tag{1}$$

To satisfy the optimum -3 dB power transfer to each balanced port, the required coupling factor is -4.8 dB. Based on Equation (1), the theoretical return losses of the two balanced ports are -6 dB, meaning not well matched to $50\,\Omega$. However, in standard measurements, such as four-port scattering measurement, the port terminals are all calibrated to $50\,\Omega$. So, the matching networks are needed to meet the standard $50\,\Omega$ system. The Marchand balun scattering matrix then can be modified from $[S]_{core}$ to $[S]'_{Balun}$,

$$[S]'_{Balun} = \begin{bmatrix} S'_{b,11} & S'_{b,12} & S'_{b,13} \\ S'_{b,21} & S'_{b,22} & S'_{b,23} \\ S'_{b,31} & S'_{b,32} & S'_{b,33} \end{bmatrix}, \tag{2}$$

where the magnitude of $S'_{b,11}$, $S'_{b,22}$ and $S'_{b,33}$ are below -15 dB among operation frequencies. Therefore, as shown in Figure 2, the plane XX' and YY' have impedance around $50\,\Omega$.

Figure 2 depicts the proposed back-to-back testing method for the amplitude and phase balances measurement, where the two identical baluns are back-to-back connected in two different ways. The one with

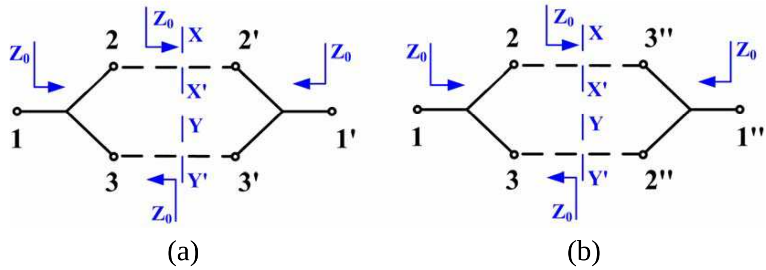

Figure 2. Block diagram of the two different back-to-back connection ways of two identical baluns. (a) The one with port 2 to port 2, port 3 to port 3. (b) The one with port 2 to port 3, port 3 to port 2.

port 2 to port $2'$ connection is shown in Figure 2(a), the other one with port 2 to port $3''$ connection is illustrated in Figure 2(b). The two-port scattering matrix of 1–$1'$ and 1–$1''$ can be obtained from standard two-port scattering measurement. Assuming the signal at port 1 is

$$s_1 = 1. \tag{3}$$

The signal transmitted to balanced ports 2 and 3 can be represented as $S'_{b,21}$ and $S'_{b,31}$, which are given by

$$S'_{b,21} = A_2 e^{-j\theta_2}, \tag{4a}$$

$$S'_{b,31} = A_3 e^{-j\theta_3}, \tag{4b}$$

where A_2 and A_3 are the normalized amplitude of signal transmitted to port 2 and port 3, respectively. θ_2 and θ_3 represent the changed phase of $S'_{b,21}$ and $S'_{b,31}$, respectively.

As illustrated in Figure 2, the signals are combined in $1'$ and $1''$, respectively. So the signal at $1'$ and $1''$, represented by $s_{1'}$ and $s_{1''}$, are obtained as

$$s_{1'} = A_2 A_{2'} e^{-j(\theta_2+\theta_{2'})} + A_3 A_{3'} e^{-j(\theta_3+\theta_{3'})}, \tag{5a}$$

$$s_{1''} = A_2 A_{3''} e^{-j(\theta_2+\theta_{3''})} + A_3 A_{2''} e^{-j(\theta_3+\theta_{2''})}. \tag{5b}$$

In this work, two identified baluns have been adopted in back-to-back connection. So it can be deduced that

$$A_{2''} = A_{2'} = A_2, \tag{6a}$$

$$\theta_{2''} = \theta_{2'} = \theta_2, \tag{6b}$$

$$A_{3''} = A_{3'} = A_3, \tag{6c}$$

$$\theta_{3''} = \theta_{3'} = \theta_3. \tag{6d}$$

With these conditions, the Equations (5a) and (5b) can be simplified as

$$s_{1'} = A_2^2 e^{-2j\theta_2} + A_3^2 e^{-2j\theta_3}, \tag{7a}$$

$$s_{1''} = 2A_2 A_3 e^{-j(\theta_2+\theta_3)}. \tag{7b}$$

Then we can get that

$$s_{1'} + s_{1''} = \left(A_2 e^{-j\theta_2} + A_3 e^{-j\theta_3}\right)^2, \tag{8a}$$

$$s_{1'} - s_{1''} = \left(A_2 e^{-j\theta_2} - A_3 e^{-j\theta_3}\right)^2. \tag{8b}$$

Derived from the Equations (8a) and (8b), the S-parameters of the two balanced ports of the balun can be written as

$$S'_{b,21} = A_2 e^{-j\theta_2} = \frac{\sqrt{s_{1'} + s_{1''}} \pm \sqrt{s_{1'} - s_{1''}}}{2}, \tag{9a}$$

$$S'_{b,31} = A_3 e^{-j\theta_3} = \frac{\sqrt{s_{1'} + s_{1''}} \mp \sqrt{s_{1'} - s_{1''}}}{2}. \tag{9b}$$

Mathematically, there are four sets of solutions fitting for Equations (9a) and (9b),

$$\begin{cases} S'_{b,21} = \dfrac{\left|\sqrt{s_{1'} + s_{1''}}\right| e^{-j\theta_b} + \left|\sqrt{s_{1'} - s_{1''}}\right| e^{-j\theta_c}}{2} \\ S'_{b,31} = \dfrac{\left|\sqrt{s_{1'} + s_{1''}}\right| e^{-j\theta_b} - \left|\sqrt{s_{1'} - s_{1''}}\right| e^{-j\theta_c}}{2} \end{cases}, \tag{10a}$$

$$\begin{cases} S'_{b,21} = \dfrac{\left|\sqrt{s_{1'} + s_{1''}}\right| e^{-j\theta_b} - \left|\sqrt{s_{1'} - s_{1''}}\right| e^{-j\theta_c}}{2} \\ S'_{b,31} = \dfrac{\left|\sqrt{s_{1'} + s_{1''}}\right| e^{-j\theta_b} + \left|\sqrt{s_{1'} - s_{1''}}\right| e^{-j\theta_c}}{2} \end{cases}, \tag{10b}$$

$$\begin{cases} S'_{b,21} = \dfrac{\left|\sqrt{s_{1'} + s_{1''}}\right| e^{-j\theta_b} + \left|\sqrt{s_{1'} - s_{1''}}\right| e^{-j\theta_c}}{2} e^{j\pi} \\ S'_{b,31} = \dfrac{\left|\sqrt{s_{1'} + s_{1''}}\right| e^{-j\theta_b} - \left|\sqrt{s_{1'} - s_{1''}}\right| e^{-j\theta_c}}{2} e^{j\pi} \end{cases}, \tag{10c}$$

$$\begin{cases} S'_{b,21} = \dfrac{\left|\sqrt{s_{1'} + s_{1''}}\right| e^{-j\theta_b} - \left|\sqrt{s_{1'} - s_{1''}}\right| e^{-j\theta_c}}{2} e^{j\pi} \\ S'_{b,31} = \dfrac{\left|\sqrt{s_{1'} + s_{1''}}\right| e^{-j\theta_b} + \left|\sqrt{s_{1'} - s_{1''}}\right| e^{-j\theta_c}}{2} e^{j\pi} \end{cases}, \tag{10d}$$

where θ_b and θ_c represent the angles of $(s_{1'} + s_{1''})^{1/2}$ and $(s_{1'} - s_{1''})^{1/2}$, respectively. The solution (10c) has an 180° phase difference with solution (10a) and the solution (10d) differs from solution (10b) with an 180° phase difference. According to Equation (1), with the port number sequences defined in Figure 1, the relative phase of

S_{21} is about 90° surpass S_{11} and the relative phase of S_{31} is about 90° after S_{11} at the operation frequencies. Under such condition, solutions (10a) and (10c) could not be compatible at the same time. Also solutions (10b) and (10d) could not be valid simultaneously. Hence, only two of the four sets solutions are fit for the Marchand balun. To distinguish the reasonable set of solution between the two possible sets of solutions, the physical asymmetric property of Marchand balun need to be considered. For an ideal Marchand balun, S_{21} and S_{31} are of the same magnitude and the 180° phase difference. However, the physical implementation of Marchand balun could not be symmetric, which makes the amplitude and phase differences of the two balanced ports shifting from 0 and 180°, respectively. Therefore, from [17, 18] or simulation results could feature such trends of shifting in S_{21} and S_{31} curves, where the reasonable solution could be identified. The amplitude and phase imbalances, represented as AM and PM, can be derived from Equations (9a) and (9b),

$$AM = abs\left[A_2 - A_3\right], \tag{11a}$$

$$PM = abs\left[\theta_2 - \theta_3\right]. \tag{11b}$$

3. VIALESS IMPLEMENTATION AND EXPERIMENTAL RESULTS

Figure 3 shows the top-view photograph of the fabricated vialess Marchand balun with two kinds of different back-to-back connections, which are optimally designed by the Ansoft HFSS and fabricated on the quartz substrate with a thickness of 0.127 mm and a dielectric constant of 3.78.

The balun patterns are formed by photolithography and magnetron sputtering method. Liftoff technology is used to remove unnecessary metals. Samples are soaked in chlorobenzene before developing, which makes it easier for liftoff. Titanium (Ti)/gold layers with the thickness of 10/100 nm are deposited on the quartz substrate as seed layers. Ti layer is used to ensure a good adhesion to the substrate. Gold of 3 μm is electroplated on the seed layers to form the balun.

As for V-band application, the strip and slot widths of the central two coupled lines in a Marchand balun are 50 μm and 10 μm, respectively. The lengths of the two coupled lines are around one quarter-wavelength of 60 GHz and optimized for the amplitude and phase balances. Microwave radius stubs are adopted to substitute the via-holes, which in additionally can provide DC isolation in all three terminals. The radius and angle of the microwave radial stub is 500 μm and 45°, respectively.

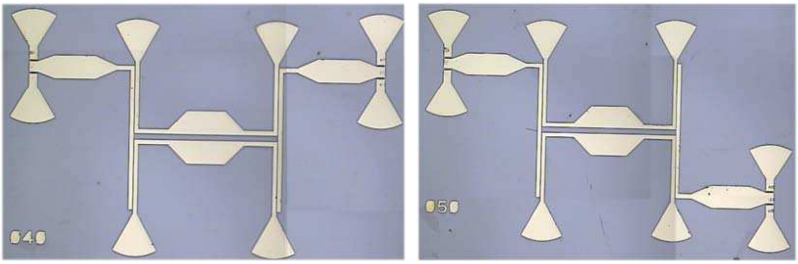

(a) (b)

Figure 3. Microphotographs of the two different back-to-back connection ways of two identical baluns. (a) The one with port 2 to port 2, port 3 to port 3. (b) The one with port 2 to port 3, port 3 to port 2.

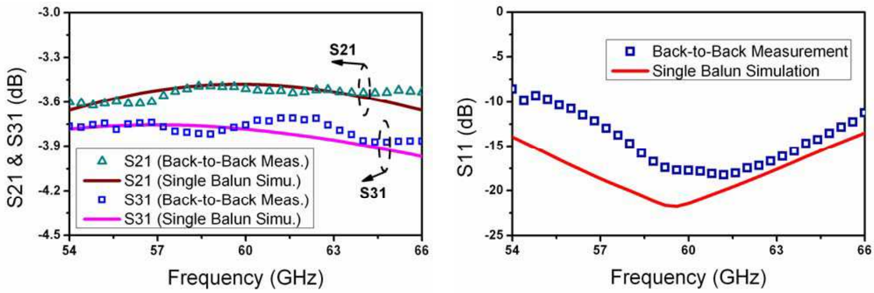

(a) (b)

Figure 4. The extracted S-parameter results from the two back-to-back measurements and compared with single balun simulated results. (a) S_{21} and S_{31}. (b) S_{11}.

The two identical vialess baluns are fabricated back-to-back with two different connections, which are featured in Figure 3. The two port S-parameters of back-to-back balun in Figures 3(a) and 3(b) are measured by Agilent PNA N5425A network analyzer and the pad effective has been de-embedded.

Figure 4(a) illustrates the magnitude response of S_{21} and S_{31} of a single vialess Marchand balun derived from the measured results of the two different back-to-back balun transitions by the proposed method in II, whereas compared with the simulation results of the single vialess Marchand balun. The results match well with each other, showing insertion losses around $-3.6\,\text{dB}$ and $-3.8\,\text{dB}$, respectively, ranging from 54 GHz to 66 GHz. The deviations between the calculations using the proposed method and the single simulation results are less than 0.15 dB, so as to make up the method with a reasonable good performance.

As featured in Figure 4(b), the magnitude responses of S_{11} in back-to-back measurement and single Marchand balun are matched well with each other. Both are lower than -10 dB from 54 GHz to 66 GHz, which provides good performance in unbalanced port return loss.

The amplitude and phase imbalances are plotted in Figures 5(a) and 5(b). The results show the amplitude difference and phase difference between port 2 and port 3 are less than 0.3 dB and 2° from 54 GHz to 66 GHz, respectively, indicating good amplitude and anti-phase balances.

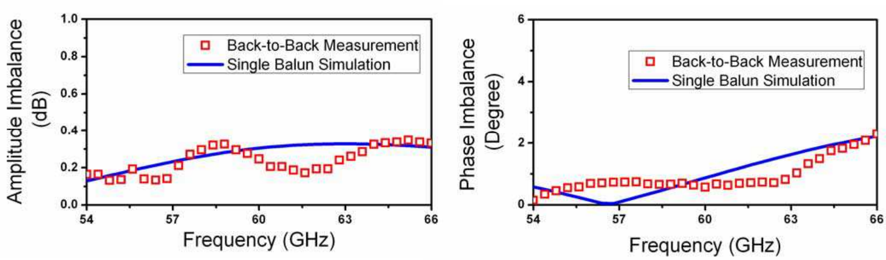

(a) (b)

Figure 5. The extracted amplitude and phase imbalances from the two back-to-back measurements and compared with single balun simulated results. (a) Amplitude imbalance. (b) Phase imbalance.

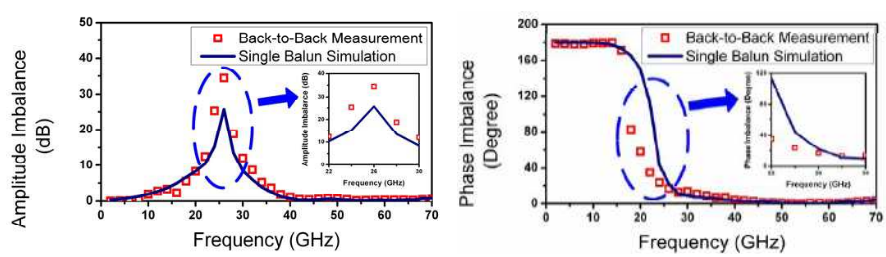

(a) (b)

Figure 6. The extracted amplitude and phase imbalances from the two back-to-back measurements and compared with single balun simulated results from 2 GHz to 70 GHz. (a) Amplitude imbalance. (b) Phase imbalance.

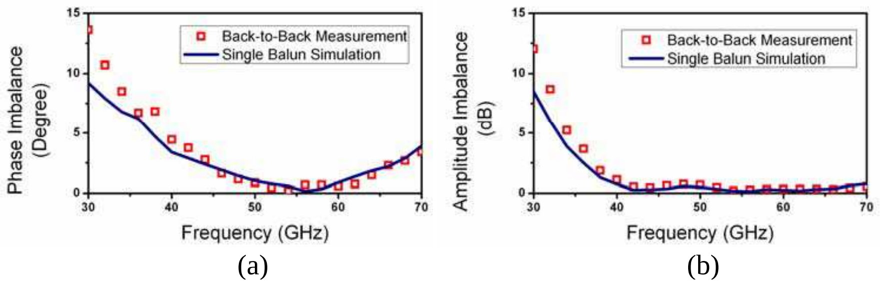

Figure 7. The extracted amplitude and phase imbalances from the two back-to-back measurements and compared with single balun simulated results from 30 GHz to 70 GHz. (a) Amplitude imbalance. (b) Phase imbalance.

There is some limitation in the implementation of this back-to-back measurements method. As shown in Figures 6(a) and (b), the amplitude and phase imbalances are plotted from 2 GHz to 70 GHz, in which the trends of curves derived from the proposed method are in good accordance with the single balun simulation. However, the curves show that the deviations between the proposed method and single balun simulations are more determined by the amplitude imbalance but less by the phase imbalance. The figures of amplitude and phase imbalances from 22 GHz to 30 GHz indicate that when the amplitude imbalance is larger than about 7 dB, the accuracy of this method could not be guaranteed. As described in Figure 7, the amplitude imbalance should be less than 2 dB to keep a less than 0.5 dB and 5 degree deviations in amplitude and phase imbalances when adopting the back-to-back measurement method. The results derived from the back-to-back measurements using the proposed method are in good agreement with the simulation results, which indicates that the proposed back-to-back measured method could be an effective substitute of the standard measurements, such as four-port scattering measurement.

4. CONCLUSION

A unique-planar vialess Marchand balun consisting of radial stubs for V-band application is presented. The balun can achieve less than 2° phase imbalance and 0.3 dB amplitude imbalance from 54 GHz to 60 GHz. The novel back-to-back measured method has been proposed and analyzed, in which the amplitude and phase imbalances can be derived from the measured back-to-back two-port scattering results. The extracted amplitude and phase imbalances achieve good agreement with the single balun simulation results. Compared with conventional Marchand balun with via-holes, this balun configuration lowers the cost, facilitates the fabrication, achieves good yield and eases the assembling. What's more, the novel measured method can decrease the cost for four-port measurement testing. Both of which are attractive for higher millimeter-wave frequencies circuit applications.

ACKNOWLEDGMENT

This work is supported by National Science and Technology Major Project (No. 2011ZX0300400202).

REFERENCES

1. Lai, Y.-A., C.-N. Chen, and Y.-H. Wang, "Compact doubler with simple harmonics suppression and gain-compensation functions," *IEEE Microw. Wireless Compon. Lett.*, Vol. 21, No. 7, 371–373, Jul. 2011.
2. Yang, H.-Y., J.-H. Tsai, T.-W. Huang, and H. Wang, "Analysis of a new 33–58 GHz doubly balanced drain mixer in 90-nm CMOS technology," *IEEE Trans. Microw. Theory Tech.*, Vol. 60, No. 4, 1057–1068, Apr. 2012.
3. Chiou, H.-K. and J.-Y. Lin, "Balanced mixers using wideband symmetric offset strack balun in 0.18 μm CMOS," *Progress In Electromagnetics Research C*, Vol. 23, 41–54, 2011.
4. Lee, J.-W., L. F. Eastman, and K. J. Webb, "A Gallium-Nitride push-pull microwave power amplifier," *IEEE Trans. Microw. Theory Tech.*, Vol. 51, No. 11, 2243–2249, Nov. 2003.
5. Marchand, N., "Transmission line conversion transformers," *Electronics*, Vol. 17, No. 12, 142–145, Dec. 1944.
6. Chongcheawchamnan, M., C. Y. Ng, K. Bandudej, A. Worapishet, and I. D. Robertson, "On miniaturization isolation network of an all-ports matched impedance-transforming marchand balun," *IEEE Microw. Wireless Compon. Lett.*, Vol. 13, No. 7, 281–283, Jul. 2003.
7. Shao, J., H. Zhang, C. Chen, S. Tan, and K. J. Chen, "A compact dual-band coupled-line balun with tapped open-ended stubs," *Progress In Electromagnetics Research C*, Vol. 22, 109–122, 2011.
8. Kidera, N., S. Watanabe, K. Watanabe, S. Pinel, and J. Laskar, "Wideband, low loss and compact 3D LTCC balun with asymmetric structure for millimeter wave applications," *2005 IEEE MTT-S Int. Microwave Symp. Dig.*, 547–550, Jun. 2005.

9. Tseng, C. H. and Y.-C. Hsiao, "A new broadband marchand balun using slot-coupled microstrip lines," *IEEE Microw. Wireless Compon. Lett.*, Vol. 20, No. 3, 157–159, Mar. 2010.
10. Lin, C.-M., C.-C. Su, S.-H. Hung, and Y.-H. Wang, "A compact balun based on microstrip EBG cell and interdigital capacitor," *Progress In Electromagnetics Research Letters*, Vol. 12, 111–118, 2009.
11. Settaluri, R. K. and A. Weisshaar, "A broadside edge coupled viasless balun," *2003 IEEE MTT-S Int. Microwave Symp. Dig.*, Vol. 2, 1251–1254, Jun. 2003.
12. Yeh, Z.-Y. and Y.-C. Chiang, "A miniature CPW balun constructed with length-reduced 3 dB couples and a short redundant transmission line," *Progress In Electromagnetics Research*, Vol. 117, 195–208, 2011.
13. Sun, S., L. Zhu, and K. S. Ang, "Multisection vialess baluns with coupled-line impedance transformers," *2006 IEEE MTT-S Int. Microwave Symp. Dig.*, 1149–1152, Jun. 2006.
14. Zhang, Z. Y., Y. X. Guo, L. C. Ong, and M. Y. W. Chia, "A new wide-band planar balun on a signle-layer PCB," *IEEE Microw. Wireless Compon. Lett.*, Vol. 15, No. 6, 416–418, Jun. 2005.
15. Sanchez-Martinez, J.-J. and E. Marquez-Segura, "Generalized analytical design of broadband planar baluns based on wire-bonded multiconductor transimission lines," *Progress In Electromagnetics Research*, Vol. 134, 169–187, 2013.
16. Ang, K. S. and Y. C. Leong, "Converting baluns into broadband impedance-transforming 180 hybrids," *IEEE Trans. Microw. Theory Tech.*, Vol. 50, No. 8, 1990–1995, Aug. 2002.
17. Mongia, R., I. Bahl, and P. Bhartia, *RF and Microwave Coupled-line Circuits*, Artech House, Norwood, MA, 1999.
18. Pozar, D. M., *Microwave Engineering*, 2nd Edition, Wiley, New York, 1998.